Measuring the lifetime of singlet oxygen in a single cell: addressing the issue of cell viability

Sonja Hatz,[a] John D. C. Lambert[b] and Peter R. Ogilby*[a]

Received 15th May 2007, Accepted 13th July 2007
First published as an Advance Article on the web 30th July 2007
DOI: 10.1039/b707313e

Singlet molecular oxygen, $O_2(a^1\Delta_g)$, has been detected from single neurons and HeLa cells in time-resolved optical experiments by its 1270 nm phosphorescence ($a^1\Delta_g \rightarrow X^3\Sigma_g^-$) upon irradiation of a photosensitizer incorporated into the cell. The cells were maintained in a buffered medium and their viability was assessed by live/dead assays. To facilitate the detection of singlet oxygen, intracellular H_2O was replaced with D_2O by an osmotic de- and rehydration process. The effect of this insult on the cells was likewise assessed. The data indicate that, in the complicated transition from a "live" to "dead" cell, the majority of our cells have the metabolic activity and morphology characteristic of a live cell. Quenching experiments demonstrate that the singlet oxygen lifetime in our cells is principally determined by interactions with intracellular water and not by interactions with other cell constituents. The data indicate that in a viable, metabolically-functioning, and H_2O-containing cell, the lifetime of singlet oxygen is ~3 μs. This is consistent with our previous reports, and confirms that the singlet oxygen lifetime in a cell is much longer than hitherto believed. This implies that, in a cell, singlet oxygen is best characterized as a selective rather than reactive intermediate. This is important when considering roles played by singlet oxygen as a signaling agent and as a component in events that result in cell death. The data reported herein also demonstrate that spatially-resolved optical probes can be used to monitor selected events in the light-induced, singlet-oxygen-mediated death of a single cell.

Introduction

Singlet molecular oxygen ($a^1\Delta_g$) is the lowest excited electronic state of molecular oxygen, and is an intermediate in many oxidative degradation reactions.[1,2] These oxidation reactions can be involved in processes that range from the degradation of organic polymers to a plethora of biological mechanisms.[3,4] Over the last 20–30 years, there has been a great deal of interest in the roles played by singlet oxygen in photo-induced processes in both plant and animal cells. Particular attention has been focused on photo-induced events that result in cell death.[5,6] In these circumstances, appreciable amounts of singlet oxygen are generally produced by the process of photosensitization; upon irradiation of a molecule (*i.e.*, the sensitizer) that is either endogenous to the system or that is specifically added for this purpose, energy transfer from the photoexcited sensitizer to ground state oxygen ($X^3\Sigma_g^-$) results in the production of singlet oxygen. Ample evidence has been provided to indicate that singlet oxygen indeed promotes cell death in such photosensitized systems.[6–8] The photo-initiated, singlet-oxygen-mediated death of cells has been exploited in a number of ways, ranging from photodynamic cancer therapies[9] to anti-bacterial treatments.[10,11]

Over the years, increasingly sophisticated optical techniques have been employed to monitor singlet oxygen from bulk ensembles of cells and from model solutions of cell constituents.[12–14] We have recently demonstrated that singlet oxygen can be optically detected from a single cultured neuron upon irradiation of a sensitizer incorporated into the cell. In this work, singlet oxygen was detected by its 1270 nm $a^1\Delta_g \rightarrow X^3\Sigma_g^-$ phosphorescence in both steady-state[15] and time-resolved experiments.[16–18] Moreover, using a focused laser beam, we could confine sensitizer excitation to small sub-cellular spatial domains.[16–18] The principal feature of this work is that we can now selectively create and directly detect singlet oxygen at the sub-cellular level in a single cell. This has far reaching implications from the perspective that singlet oxygen is a key intermediate, if not *the* key intermediate, involved in both apoptotic and necrotic mechanisms of photo-induced cell death.[6–8]

We have thus far performed a wide range of singlet oxygen experiments on single cells under a variety of conditions using both steady-state irradiation of a whole cell as well as pulsed femtosecond laser irradiation in selected sub-cellular domains.[15–18] Through this work, we consistently ascertained that, with the cells used in our studies and under our experimental conditions, the lifetime of intracellular singlet oxygen was much longer than what has been commonly believed for the past ~25 years. Our data indicated that the lifetime of singlet oxygen in the cells studied was principally determined by interactions with the water in the cell and not by interactions with other cell constituents. Given the diversity of intracellular constituents, this is perhaps a surprising observation. Nevertheless, a variety of potentially complementary explanations might account for this phenomenon. For example, proteins in the cell could exist in conformations that are not conducive to the efficient quenching of singlet oxygen (*i.e.*, key functional moieties such as nitrogen lone pairs and thiol groups are shielded). This particular suggestion is consistent with data published by Michaeli and Feitelson[19] who have shown that

[a]*Department of Chemistry University of Aarhus, DK-8000, Århus, Denmark. E-mail: progilby@chem.au.dk*
[b]*Department of Physiology University of Aarhus, DK-8000, Århus, Denmark*

proteins in their native state are indeed poorer quenchers of singlet oxygen than denatured proteins.

This low level of intracellular singlet oxygen reactivity, as manifested in a long singlet oxygen lifetime, suggests that singlet oxygen will exhibit more selectivity in its reactions. These could include redox reactions (*i.e.*, the formation of the superoxide ion and an organic radical cation) and the formation of peroxides, and could have a spatially-resolved component depending on the distribution of potential reaction partners in the cell. Of course, the comparatively long lifetime of intracellular singlet oxygen also indicates that it will diffuse over a greater distance in the cell before deactivation, and its sphere of potential activity within the cell will be correspondingly greater than previously believed. This low reactivity and comparatively large diffusion distance are consistent with the observation that the decay of singlet oxygen within our cells follows first-order kinetics. Thus, through diffusion and multiple collisions, the intracellular environment experienced by singlet oxygen is effectively homogeneous. Clearly, all of these points can have important ramifications in interpreting the roles played by singlet oxygen in mechanisms of both cell signaling and cell death.

In our single-cell experiments thus far, we have focused on working with systems which were most conducive, or which we believed were most conducive, to the generation of a detectable singlet oxygen phosphorescence signal. One of the most significant constraints imposed was the exchange of intracellular H_2O with D_2O. Through this process, we wanted to capitalize on the fact that the lifetime of singlet oxygen in quencher-free D_2O ($\tau_\Delta \sim 68$ μs[20]) is ~20 times longer than that in H_2O ($\tau_\Delta \sim 3.5$ μs[21–23]) which is reflected in a quantum efficiency of singlet oxygen phosphorescence that is much larger in D_2O than in H_2O. Indeed, the very fact that we can exploit this solvent isotope effect in our work indicates that endogenous quenchers do not effectively compete with the solvent in processes that deactivate singlet oxygen in the cell.

To exchange H_2O with D_2O, cells were subjected to an osmotic shock. First we used a hypertonic extracellular medium to extract the majority of intracellular H_2O, followed by exposure to an isotonic D_2O-containing medium, to "rehydrate" the cells.[15,24] We also avoided using common biological buffers and supporting media containing compounds that we believed might quench or otherwise deactivate singlet oxygen. Rather, our cells were exposed only to a minimal maintenance medium containing NaCl, KCl, and glucose for the periods of up to 5–7 hours during which the cells were loaded with D_2O and the sensitizer and the optical experiments were performed.[16,17,24]

The osmotic shock, the presence of D_2O in the cell, the use of a minimal maintenance medium, and the presence of a sensitizer incorporated into the cell could all adversely affect the cells such as to yield anomalous singlet oxygen data. Although our previous optical experiments were always performed on intact cells that appeared to be healthy and viable as viewed through a bright-field microscope, the perturbations listed above certainly do not help to assuage the skeptic regarding the general biological significance of our results.

With these points in mind, we set out to repeat our photosensitized singlet oxygen optical experiments using cells maintained in a standard physiological buffer and whose viability was assessed using standard live/dead assays. We also set out to determine the generality of our results by performing experiments on cells other than rat neurons obtained from primary cultures. To this end, complementary experiments were performed using cells from the HeLa line.

Materials and methods

Cell preparation

Cultures of neurons were prepared from the hippocampus of Wistar rat embryos as outlined elsewhere.[24,25] HeLa cells were grown in a CO_2 incubator at 37 °C in a standard culturing/growth medium (Dulbecco's modified Eagle's medium containing 10% fetal calf serum and antibiotics). For plating onto cover slips, the cells were first rinsed with phosphate buffered saline and trypsinated (0.5% trypsin). After 20 min, the cells were collected and washed twice with the culturing medium. The cells were resuspended in the culturing medium and plated onto cover slips coated with poly-D-lysine. Experiments on the cells were performed only after a period of 24 h to allow the cells to attach to the cover slips.

Minimal Maintenance Medium (MMM)

This medium was used in all of our earlier singlet oxygen studies, and for selected control experiments in the present work. The MMM is an aqueous solution of 140 mM NaCl, 3.5 mM KCl, and 10 mM glucose prepared using either D_2O, H_2O, or mixtures of D_2O and H_2O.

Standard Maintenance Medium (SMM)

This is a buffered, physiologically compatible medium that has been used for electrophysiological recordings from cells.[26] The SMM is an aqueous solution of 140 mM NaCl, 3.5 mM KCl, 2 mM $CaCl_2$, 2 mM $MgCl_2$, 1.25 mM NaH_2PO_4, 10 mM glucose, and 10 mM HEPES (*i.e.*, 4-(2-hydroxyethyl)-1-piperazine-ethanesulfonic acid) prepared using either D_2O, H_2O, or mixtures of D_2O and H_2O. The pH of this solution was adjusted to 7.35 using NaOH and the osmolarity was adjusted to 310 mosmol using sucrose. When used, the culturing medium was replaced with the SMM for the course of the optical experiments. HEPES (>99.5%, Sigma) was used as received for the preparation of the SMM, but was dried at 80 °C for 18 h under vacuum prior to use in the singlet oxygen quenching studies.

Protocol for H_2O/D_2O exchange and sensitizer incorporation

The following steps were taken to exchange the intracellular H_2O with D_2O (or mixtures of D_2O and H_2O) and to incorporate the sensitizer. For all of the work reported here, the sensitizer used was 5,10,15,20-tetrakis(*N*-methyl-4-pyridyl)-21*H*,23*H*-porphine, TMPyP (obtained from Aldrich as the tetra-*p*-tosylate salt and used as received). (1) The cover slip containing the cells was removed from the culture/growth medium and washed with an isotonic H_2O-based solution of either MMM or SMM. (2) The cells were incubated for 5 min with a hypertonic (584 mosmol) D_2O-based solution of MMM prepared with 280 mM NaCl, 7 mM KCl, and 10 mM glucose. (3) The cells were washed three times with a D_2O-based solution prepared as in step (1). (4) The cells

were held in a CO_2 incubator at 37 °C for 24 h in an isotonic D_2O solution of either MMM or SMM that contained 10 μM TMPyP. (5) The cells were washed three times with an isotonic D_2O-based solution of either MMM or SMM.

Viability assays

Four established assays were used to test cell viability. Unless otherwise indicated, assays were performed under air and we excluded as much ambient light as possible.

Propidium iodide (PI) assay. Cells were incubated for 30 min in solutions of either SMM or MMM containing 4 μM PI, after which the cells were washed with either SMM or MMM to remove the excess PI. Uptake of PI was monitored in a fluorescence imaging experiment (excitation λ of 535 nm, detection λ of 650 nm). In a typical experiment, ~150–250 cells were examined. Control experiments were performed on the same day using cells from the same batch. PI (Sigma Aldrich) was used as received.

Rhodamine 123 (Rh123) assay. Cells were incubated for 30 min in solutions of either SMM or MMM containing 20 nM Rh123, after which the cells were washed with either SMM or MMM to remove the excess Rh123. Fluorescence of Rh123 from the cells was monitored in an imaging experiment (excitation λ of 480 nm, detection λ of 535 nm). Rh123 (Sigma Aldrich) was used as received.

Fast halo assay. The general procedure of Sestili, *et al.*[27] was followed. Briefly, cells were placed on a cover slip that had a raised perimeter (Frameseal™, Sigma Aldrich). 600 μl 1% low melting point agarose (Sigma Aldrich) in either SMM or MMM was added, and the gel was allowed to set at room temperature for 30 min. Addition of 1 ml of 0.3 M NaOH lysed the cells and, after 30 min, the gel was neutralized by the addition of 0.4 M TRIS buffer at pH 7.6. A solution of 4 μM PI in either MMM or SMM was then added to stain the DNA. Control experiments included performing the fast halo assay on cells in which apoptosis had been initiated by incubation with 0.1 mg ml^{-1} of camptothecin for 3 h at 37 °C in a CO_2 incubator.

MTT assay. The procedure of Nikkhah *et al.*[28] was followed. Cells were incubated for 4 h at 37 °C in a CO_2 incubator in a solution of either MMM or SMM containing 1 mg ml^{-1} MTT [*i.e.*, 3-(4,5-dimethylthiazol-2-yl)-2,5-diphenyltetrazolium bromide]. Cells were imaged under bright field illumination to visualize crystals of reduced MTT. DMSO was used as the solvent for the independent experiments in which the reduced MTT was extracted from the cells. MTT (Sigma Aldrich) was used as received.

Instrumentation

Details of the instrumentation and approach used in this study are provided elsewhere.[16–18,29] Briefly, cells to be studied were contained in an atmosphere-controlled chamber that was mounted onto the translation stage of an inverted microscope. Subsequent steps of irradiation and optical monitoring varied depending on the experiment.

For the singlet oxygen experiments, the sensitizer that had been incorporated into the cell, TMPyP, was irradiated using the output of a femtosecond laser system that had been focused into the cell using the microscope objective. The irradiation wavelength was 420 nm which coincides with the Soret absorption band of TMPyP. The laser was operated at a repetition rate of 1 kHz with an energy of 10 nJ $pulse^{-1}$, which was measured prior to coupling the beam into the microscope optics. Singlet oxygen phosphorescence was collected using the microscope objective, spectrally isolated using a 1270 nm interference filter, and transmitted to a cooled IR photomultiplier tube operated in a photon counting mode. Time-resolved signals were recorded by successively increasing the delay time between the irradiating laser pulse and the sampling window of the photon counter.

Fluorescence imaging experiments used in the viability assays were performed by irradiating the cell and its surroundings with a steady-state Xe lamp using interference filters to select the wavelength appropriate for the fluorophore in that particular assay. Light emitted by the sample was detected through interference filters using a CCD camera (Evolution QEi controlled by ImagePro software, Media Cybernetics) placed at the image plane of the microscope. Bright-field images were recorded using the same CCD camera; back-lighting was achieved with a tungsten lamp provided as an accessory to our Olympus IX70 inverted microscope.

Results and discussion

Quenching of singlet oxygen by HEPES

The amine HEPES (Fig. 1(a)) is well tolerated by biological systems and, with its pK_a of 7.5, is extensively used as a buffer to maintain cells at their physiological pH.[30,31] However, aliphatic amines can be very good quenchers of singlet oxygen.[32] For this reason, we avoided using an amine-based buffer in our original work with singlet oxygen in cells (see composition of MMM, *vide supra*).[15–18]

With our current interest in using cells that are demonstrably viable, we set out to investigate if singlet oxygen phosphorescence experiments could be performed on cells in a medium that contains a relevant amount of HEPES. To this end, we first performed experiments to quantify the rate constant for singlet oxygen quenching by HEPES. Given that the quenching of singlet oxygen by amines involves charge transfer from the nitrogen lone pair to singlet oxygen,[32,33] the expectation is that the quenching rate constant should be comparatively small at pH values where a greater fraction of the amines are protonated. On the other hand, the quenching rate constant should be larger under alkaline conditions where the amine exists as the free base and where charge transfer from the amine lone pair to singlet oxygen can occur more readily.

For these experiments, D_2O solutions of TMPyP were prepared and the overall rate constant k_Δ for singlet oxygen deactivation (*i.e.*, the reciprocal of the singlet oxygen lifetime, τ_Δ^{-1}) was measured as a function of the amount of added HEPES. In such an experiment, k_Δ should be equal to the sum of the rate constant for singlet oxygen deactivation in the absence of the added quencher, k_Δ^0, and the quenching term, $k_q[Q]$, where k_q is the bimolecular rate constant for deactivation by HEPES and [Q] is the concentration of added HEPES (eqn (1)).

$$k_\Delta = k_\Delta^0 + k_q[Q] \quad (1)$$

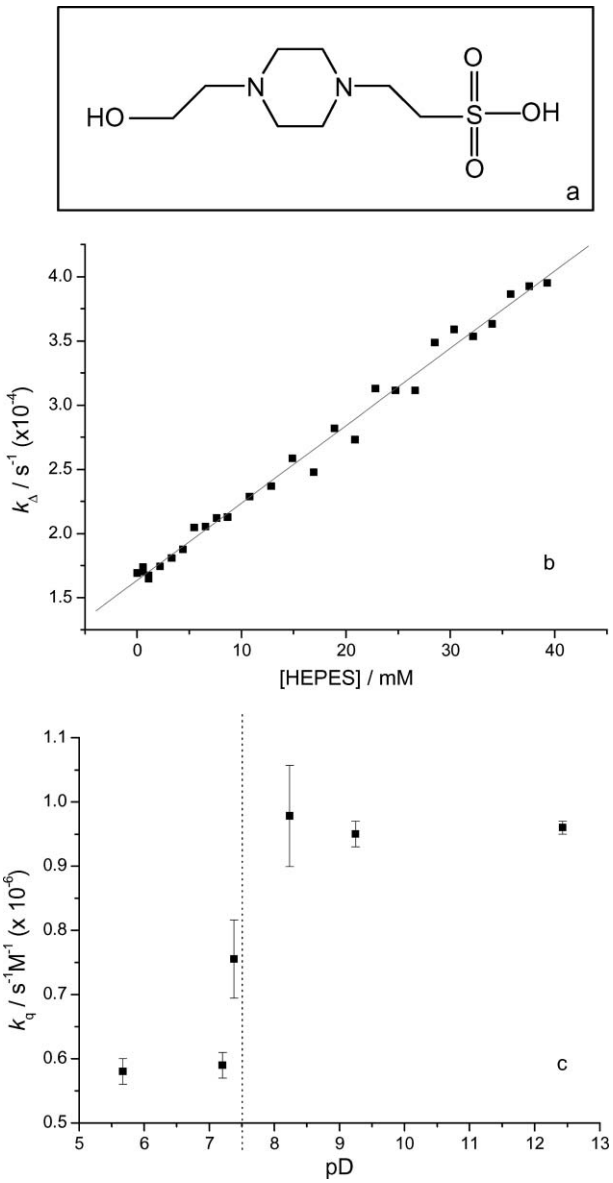

Fig. 1 (a) Structure of HEPES. (b) Plot of the overall rate constant for singlet oxygen deactivation, k_Δ, against the concentration of HEPES. These data were recorded using D_2O solutions at a pD of 7.2 and yield $k_q = (6.0 \pm 0.1) \times 10^5$ s^{-1} M^{-1}. (c) Values of k_q, the rate constant for deactivation of singlet oxygen by HEPES, are plotted against the pD of the D_2O solutions in which the experiments were performed. Each point on this plot represents an average of data recorded from several experiments. The dashed vertical line indicates the pK_a of HEPES.

The data indeed behave according to eqn (1), with plots of k_Δ against [Q] yielding values of the quenching rate constant k_q from the slope (Fig. 1(b)). Moreover, values of k_q thus obtained varied with pH in the expected manner: at pH values smaller than 7.3, $k_q = (5.8 \pm 0.1) \times 10^5$ s^{-1} M^{-1}, whereas in alkaline solutions $k_q = (9.5 \pm 0.1) \times 10^5$ s^{-1} M^{-1} (Fig. 1(c)).

Most importantly, however, we find that these values of k_q are not extraordinarily large and that HEPES is, in fact, a comparatively poor quencher of singlet oxygen in aqueous solutions. Furthermore, an analogous quenching study in which aliquots of SMM were added to D_2O indicates that HEPES is the only significant quencher of singlet oxygen in this medium. Thus, at the concentration of HEPES used in the preparation of our SMM, 10 mM, the lifetime of singlet oxygen in D_2O solutions is only moderately affected (*i.e.*, τ_Δ in neat D_2O is 68 μs,[20] and the presence of HEPES in SMM reduces τ_Δ to ~48 μs).

In conclusion, the use of a HEPES-based buffer should not adversely affect an experiment to optically detect intracellular singlet oxygen. Of course, if HEPES is not appreciably incorporated into the cell but remains mostly in the extracellular environment,[31] then the conditions for our experiments only become more favorable.

Assays for cell viability

Because the response of a cell to a given perturbation is invariably quite complicated and involves different organelles and regulatory pathways,[34] it is essential to employ a range of assays that test for different cellular responses to the perturbation. For the present work, the following four assays were used:

(a) The propidium iodide (PI) assay tests for the integrity of the cell membrane. A fully functioning membrane excludes PI from the cell. However, a dysfunctional or compromised membrane admits the red-fluorescing PI into the cell where it binds with DNA in the nucleus. Thus, a cell that has a red fluorescent nucleus in the PI assay is considered "dead". Since the plasma membrane generally ceases to function only during the final stages of the apoptotic cascade,[34] this is an assay for an advanced stage of cell death.

(b) The rhodamine 123 (Rh123) assay exploits the fact that the fluorescent dye Rh123 is membrane permeable and that it accumulates in the mitochondria of live cells as a result of the mitochondrial trans-membrane potential.[34,35] An early event in the apoptotic cascade is the loss of this mitochondrial potential which, in turn, is reflected in the delocalization of Rh123. Thus, an early and important indication that the cell's metabolic machinery may be perturbed appears as a rather diffuse Rh123 fluorescence from the cell. Granular-appearing fluorescence is indicative of viable mitochondria in which Rh123 is localized.

(c) The fast halo assay (FHA) assesses the extent to which DNA strand scission occurs in a single cell as a result of a given perturbation.[27,34] In this test, the perturbed cell and cells from the control population are first immobilized and lysed. A DNA-specific fluorescent dye (PI in our case) is then used to quantify the radial diffusion of DNA fragments away from the nucleus. Changes in the morphology of the nucleus as a result of DNA denaturation and fragmentation often occur at early stages in the apoptotic cascade and, in the FHA, this is often reflected first in a misshaped nucleus and ultimately in a fluorescent "halo" surrounding the nucleus.[27,34]

(d) The MTT assay is a test for enzymatic activity characteristic of a viable cell. In this test, a metabolically active cell will reduce 3-(4,5-dimethylthiazol-2-yl)-2,5-diphenyltetrazolium bromide (MTT) to a blue crystalline derivative, formazan, that can then be seen in a bright field microscope.[28,36] Furthermore, one can extract the formazan from the cell culture and quantify the amount produced using an absorption spectrometer, which, when compared to the amount produced by a control cell population, can be used as a measure of cell activity. Although often associated with the activity of mitochondrial dehydrogenases, it has also been shown that MTT can be reduced in cytoplasmic vesicles.[36]

Using these assays, we set out to examine if cell viability is influenced by procedures used in our singlet oxygen optical studies (note that attempts to assess photoinduced, singlet-oxygen-mediated changes in cell viability upon irradiation of a sensitizer in the cell constitute a different study). Experiments were performed on neurons as well as HeLa cells. When discussing the general response of a cell in a given assay, we occasionally refer to literature studies performed on cells in which apoptosis had been initiated. However, we do not mean to imply that corresponding results in our cells should be taken as evidence for the occurrence of apoptotic events.

It is first significant to note that the transfer of cells from the culturing to a maintenance medium (*e.g.*, our SMM) is a perturbation that, by itself, may disrupt functionality in a fraction of the cells being studied. Consequently, results of tests on the influence of D_2O, osmotic shock, and the presence of the sensitizer were compared to results obtained from two independent control populations of cells: (1) cells maintained in the culture medium, and (2) cells transferred from the culture medium to our standard H_2O-based maintenance medium (SMM).

Very few cells tolerate exposure to the minimal maintenance medium (MMM) used in our first singlet oxygen experiments on single cells.[15–18] This is clearly seen in the results of the PI assay (Fig. 2). Indeed, this result is entirely consistent with qualitative observations made during our earlier experiments; on the basis of TMPyP-based fluorescence images and bright field images, it was difficult to find a "healthy-looking" cell for study when using the MMM.

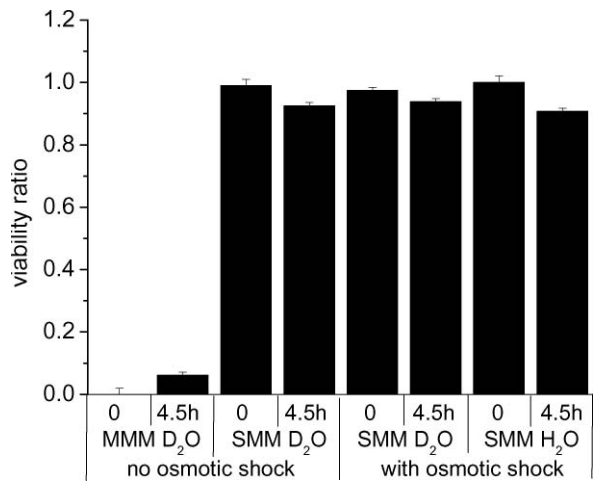

Fig. 2 Histogram showing the results of the PI assay performed on neurons. The cell viability ratio shown on the ordinate is simply the ratio of live to dead cells observed for a given test (*e.g.*, exposure to D_2O) normalized by the corresponding ratio of live to dead cells for the control population. Thus, a cell viability ratio of 1.0 indicates that the cell population under test behaves just as the control cell population. In this test, the control population was maintained in the culture medium and, on an absolute scale, an average of 8% of these cells stained dead. The effect of each perturbation was assessed by counting both live and dead cells (1) immediately after application of the perturbation (*i.e.*, at $t = 0$), and (2) 4.5 h after the application of the perturbation. Approximately 150–250 cells were counted in each test. For the SMM experiments, a one-way analysis of variance (ANOVA) with $p < 0.05$ reveals that there is no significant difference between the $t = 0$ and the $t = 4.5$ h data. Similar results were obtained from experiments performed on HeLa cells.

On the other hand, the PI data in Fig. 2 clearly show that the plasma membrane remains functionally intact for several hours in cells exposed to our standard maintenance medium (SMM). Moreover, and arguably more importantly, (1) simple exposure of the cells to D_2O, and (2) replacing intracellular H_2O with D_2O and the osmotic shock associated with this process do not have an effect on the number of cells that loose membrane function. Indeed, within the constraints of this assay, we are unable to discern any adverse effect from the use of D_2O in place of H_2O (a one-way analysis of variance, ANOVA,[37] with $p < 0.05$ reveals that there is no significant difference between the control and perturbed cell populations).

In the Rh123 assay, the manifestation of a "live" cell is a granular fluorescence image in which the mitochondria are resolved and in which the nucleus does not contain the fluorophore. In a "dead" cell, the Rh123 fluorescence is diffuse and originates principally from the nucleus where Rh123 ultimately tends to localize. In cells that have been "compromised", the Rh123 fluorescence is diffuse and it is not possible to resolve the mitochondria even though the nucleus may still appear somewhat dark. We found that it was difficult to assess the results of the Rh123 assay on neurons because these cultures are heterogeneous and contain more than one cell type in more than one layer on the cover slip (*e.g.*, glial cells that support the neurons are also present). As such, even if the Rh123 fluorescence indeed originated from the localized spatial domain of viable mitochondria, the resultant image may appear blurred because the cell might be out of the focal plane of the microscope. On the other hand, HeLa cells plate in a single layer on the cover slip and the results of the Rh123 assay are much easier to assess. Examples of the images thus obtained from HeLa cells are shown in Fig. 3.

The results of the Rh123 assay are consistent with those of the PI assay. In the Rh123 experiments, we likewise find that our cell handling procedures do not constitute major perturbations. As shown in groups 1–3 of Fig. 4, a change from the growth/culture medium to the SMM and simple exposure of the cells to D_2O does not alter the percentages of "live" and "dead" cells relative to the corresponding percentages in the control (ANOVA with $p < 0.05$ reveals that there is no significant difference in the fractions of live and dead cells in these respective cell populations).

The test results shown in groups 4–6 of Fig. 4 indicate that the osmotic shock associated with H_2O/D_2O exchange and the incorporation of TMPyP into the cell constitute more of a perturbation than the simple change from the growth medium to SMM. For the TMPyP-containing cells, the increase in the percentage of dead cells could reflect a combination of (1) the inherent toxicity of TMPyP that would be manifested in cells kept in the dark, and (2) photo-induced, singlet-oxygen-mediated death due to the adventitious exposure of the cells to the ambient room lighting during handling. Nevertheless, the majority of the cells in a given test population still indicate that they have viable mitochondrial activity and, as such, can be categorized as being "live" cells.

For our purposes, the results of the Rh123 assay can arguably be considered more important than those of the PI assay simply because the Rh123 assay is a test for events that generally occur at early stages of apoptotic cell death. In this regard, the Rh123 mitochondrial images in Fig. 3 may also reveal another response of the cell to a perturbation associated with

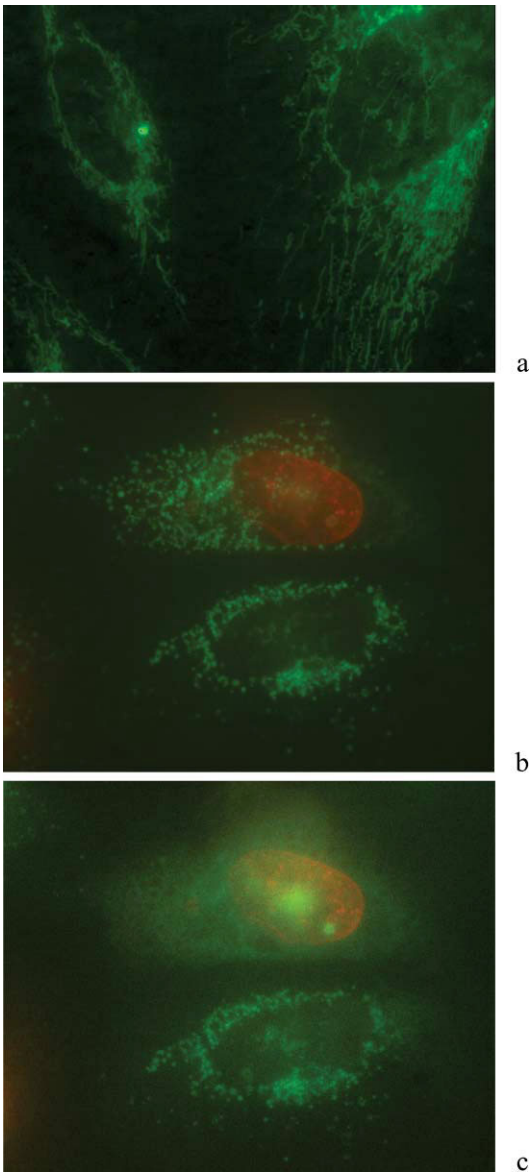

Fig. 3 Fluorescent images obtained from HeLa cells. (a) Rh123 fluorescence image from "live" cells maintained in the culture/growth medium. (b) Composite fluorescence image from two cells in the SMM that have been subjected to an osmotic shock. The green color shows the result of the Rh123 assay. This culture was also incubated with TMPyP, but only the upper cell in this image incorporated the sensitizer (note, TMPyP preferentially localizes in the cell nucleus[24,38]). This latter point is clearly documented in an image based on the fluorescence of TMPyP (red color in this image). (c) Composite fluorescence image of the same two cells shown in panel b recorded after broadband irradiation at 420 nm for 3 s using the output of a 75 W Xe lamp (*i.e.*, under our present conditions, 3 s is the time needed to record the TMPyP fluorescence image). The data clearly show that, upon irradiation at a wavelength absorbed by TMPyP, the cell containing TMPyP gives rise to a more diffuse Rh123 image which is characteristic of a "compromised" cell. Moreover, it appears that the Rh123 may be starting to accumulate in the nucleus. The cell lacking TMPyP retains the granular fluorescence characteristic of viable mitochondrial activity.

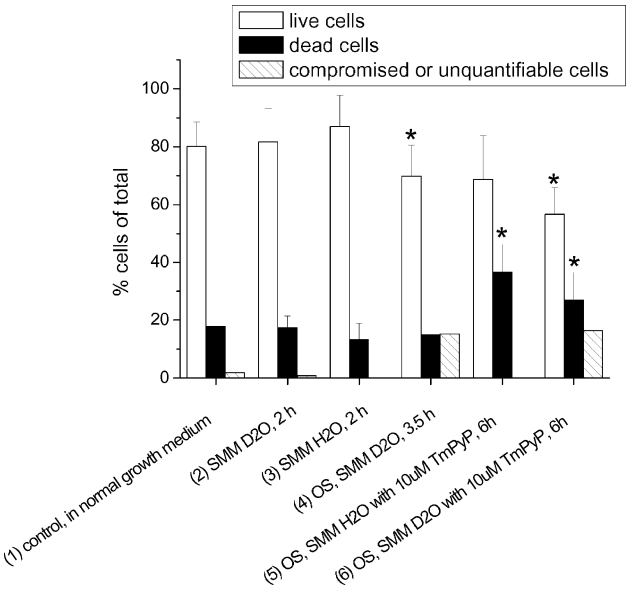

Fig. 4 Histogram showing the results of the Rh123 assay on six different HeLa cell populations. In a test on a given population, at least 1000 cells were counted using a routine available in ImageJ[39] and categorized as "live", "dead", or "compromised" (see text). Group #1 at the far left shows data from our control population in which the Rh123 assay was performed on cells in the growth/culture medium. Progressing to the right, we show data recorded under five different perturbing conditions (OS = osmotic shock, SMM = standard maintenance medium). Live/dead pylons labeled with an asterisk indicate that there is a statistically significant difference between this number and the corresponding number obtained from the control population (one-way ANOVA; $p < 0.05$). Error bars show one standard deviation. In these experiments, the number of "dead" + "live" cells was subtracted from the total number of cells (obtained from a bright field image) to yield the number of "compromised" cells.

our experiments. For Rh123 images recorded from cells in the culture medium, the mitochondria tend to be distributed in strand-like structures (Fig. 3(a)). It has been suggested that this morphology may reflect an interaction between the mitochondria and microtubules associated with the cytoskeletal network.[35,40,41] The Rh123 images in Fig. 3(b) in which the mitochondria appear as discrete cylindrical/spherical entities suggest that this putative microtubule-dependent organization is disrupted in the change from the growth/culture medium to the SMM.

The results of the MTT assay provide yet another perspective on the response of our cells to these specific perturbations. The amount of formazan extracted from the respective cell populations indicates that, by itself, the presence of TMPyP in the cell does not have a major effect on the enzymatic process by which MTT is reduced (Fig. 5). On the other hand, the combination of TMPyP incorporation and the change to the SMM results in a significant decrease in the amount of formazan produced over the 4 h incubation period. Nevertheless, evidence of cell enzymatic activity is still visible in these perturbed cells.

A potentially more interesting result of the MTT test, and one that puts the extracted formazan results of Fig. 5 into perspective, is shown in Fig. 6. In these bright field images, we clearly see that the formazan produced by control cells in the culture medium results in the formation of needle-like crystals in the extracellular medium (Fig. 6(a)). Incorporation of TMPyP into the cell does not appear to influence the production of formazan when the cells are maintained in the culture medium (*i.e.*, extracellular needle-like

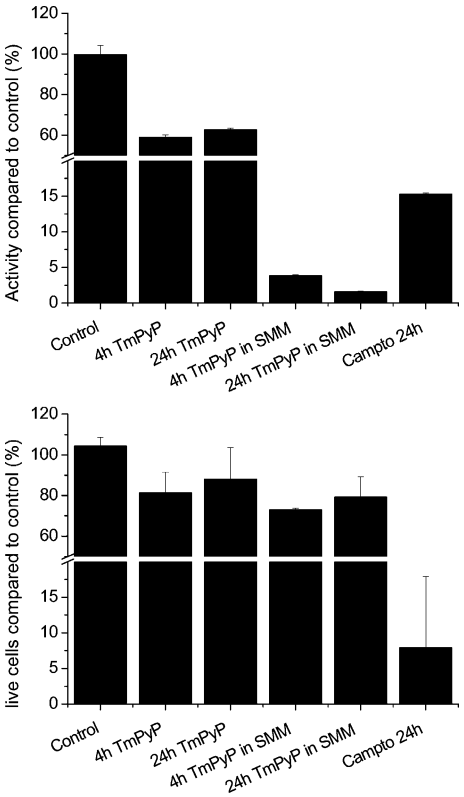

Fig. 5 Results of the MTT assay. For these experiments, cells were maintained in the culture medium unless specified as being in the SMM. Top: enzymatic activity in a given cell population as quantified by the amount of extracted formazan. The data clearly indicate that the metabolic processes assayed here are most sensitive to the change from the culture medium to SMM. The presence of TMPyP or even camptothecin, which is a DNA topoisomerase poison that promotes cell death,[30,42] did not have as large an effect as the change to SMM. Bottom: histogram that shows the results of the PI assay performed on cells exposed to MTT. In this case, the first pylon is referenced against a cell population lacking MTT.

crystals of formazan are still produced) (Fig. 6(b)). However, for cells containing TMPyP in the standard maintenance medium (SMM), the formazan that is produced exists as granules and not as extracellular needles (Fig. 6(c)). It has been demonstrated that, in the enzymatic reduction of MTT, the formazan that is produced is first deposited as intracellular granules.[36] It is only upon the migration of these granules to the cell membrane and the release of the intracellular formazan that one observes the extracellular needle-like formazan crystals on the cell surface.[36] Thus, our data seem to indicate that the transfer of our cells from the culture medium to the SMM simply slows down the dynamic processes that result in MTT uptake, reduction, and the expulsion (*i.e.*, exocytosis) of the resultant formazan.

Like the Rh123 and MTT assays, the fast halo assay (FHA) can give an indication of early events in the apoptotic cascade. This test is specific for perturbation-dependent changes in the morphology of the nucleus and for the appearance of extranuclear DNA fragments. Although the Rh123 and MTT assays clearly indicate distinct perturbations to our cells, the results of the FHA are not as well defined and systematic. In some cases, including control experiments, we were not able to observe the characteristic halo surrounding the nucleus indicative of nuclear degradation. This is illustrated in Fig. 7(a) for a cell that had been subjected to osmotic shock and incubated with D_2O for 5 h. In other cases, also including control experiments, we were able to observe a dim halo. This is shown in Fig. 7(b) for a cell that likewise had been subjected to osmotic shock. Thus, in the least, we must exercise restraint in interpreting the observation of a dim halo in our use of the FHA. Despite this caveat, we nevertheless tended to observe somewhat more pronounced halos in cells that had been incubated with TMPyP Fig. 7(c). This is consistent with reports that TMPyP can exhibit "nuclease-like" activity, even in the absence of light and oxygen.[43,44]

We conclude this discussion of viability assays with the statement that, in a given population of cells maintained in a buffered medium (*i.e.*, our SMM) and that have been prepared for a singlet oxygen experiment (*i.e.*, contain D_2O and the sensitizer TMPyP), a significant fraction show the metabolic activity and morphology characteristic of a viable cell. Of course, at the level of a single cell, the difference between "alive" and "dead" is not a clearly defined point, but rather is expressed in a range of nuances. We have provided evidence that some of our cells may indeed be "compromised" and events that result in cell death may indeed have started. Nevertheless, in the complicated and multi-step transition from "alive" to "dead", our data indicate that we are much closer to the "alive" end of the process than the "dead" end.

Singlet oxygen lifetime

Time-resolved singlet oxygen phosphorescence measurements were performed on both HeLa cells and neurons maintained in our standard buffer medium containing HEPES (*i.e.*, SMM). As in our previous studies, these single-cell experiments were performed using a microscope such that sensitizer irradiation only occurred in small sub-cellular spatial domains.[16–18,45] The sensitizer used was TMPyP which, as we have already mentioned, tends to localize in the nucleus of the cell. Singlet oxygen phosphorescence was then monitored in photon-counting experiments.

Data recorded in the present studies from metabolically-viable cells are consistent with data recorded in our earlier studies.[16–18] Specifically, the time-resolved signals obtained upon selective, spatially-resolved irradiation of the sensitizer indicate that interactions with intracellular water provide the principal channel for singlet oxygen deactivation inside a cell. The data clearly indicate that interactions with cell constituents (*e.g.*, proteins) do not dominate the deactivation of intracellular singlet oxygen. In support of these statements, we recorded the lifetime of singlet oxygen from cells that had been incubated with successively larger ratios of H_2O to D_2O. Treating H_2O as a quencher, we then plotted the data according to eqn (1) to quantify the bimolecular rate constant, k_q, responsible for the deactivation process (Fig. 8). The value obtained from the slope of the plot [$(3.0 \pm 0.7) \times 10^3$ s^{-1} M^{-1}] is close to that expected for H_2O quenching [5.2×10^3 s^{-1} M^{-1} = (3.5 μs)$^{-1}$/55 M, when 3.5 μs is taken as the lifetime of singlet oxygen in neat H_2O].

Unfortunately, within a reasonable time period of sensitizer irradiation and signal averaging, we are still not able to record a sufficiently intense time-resolved singlet oxygen signal from a single cell containing only H_2O.[29] Rather, we still need to rely on the

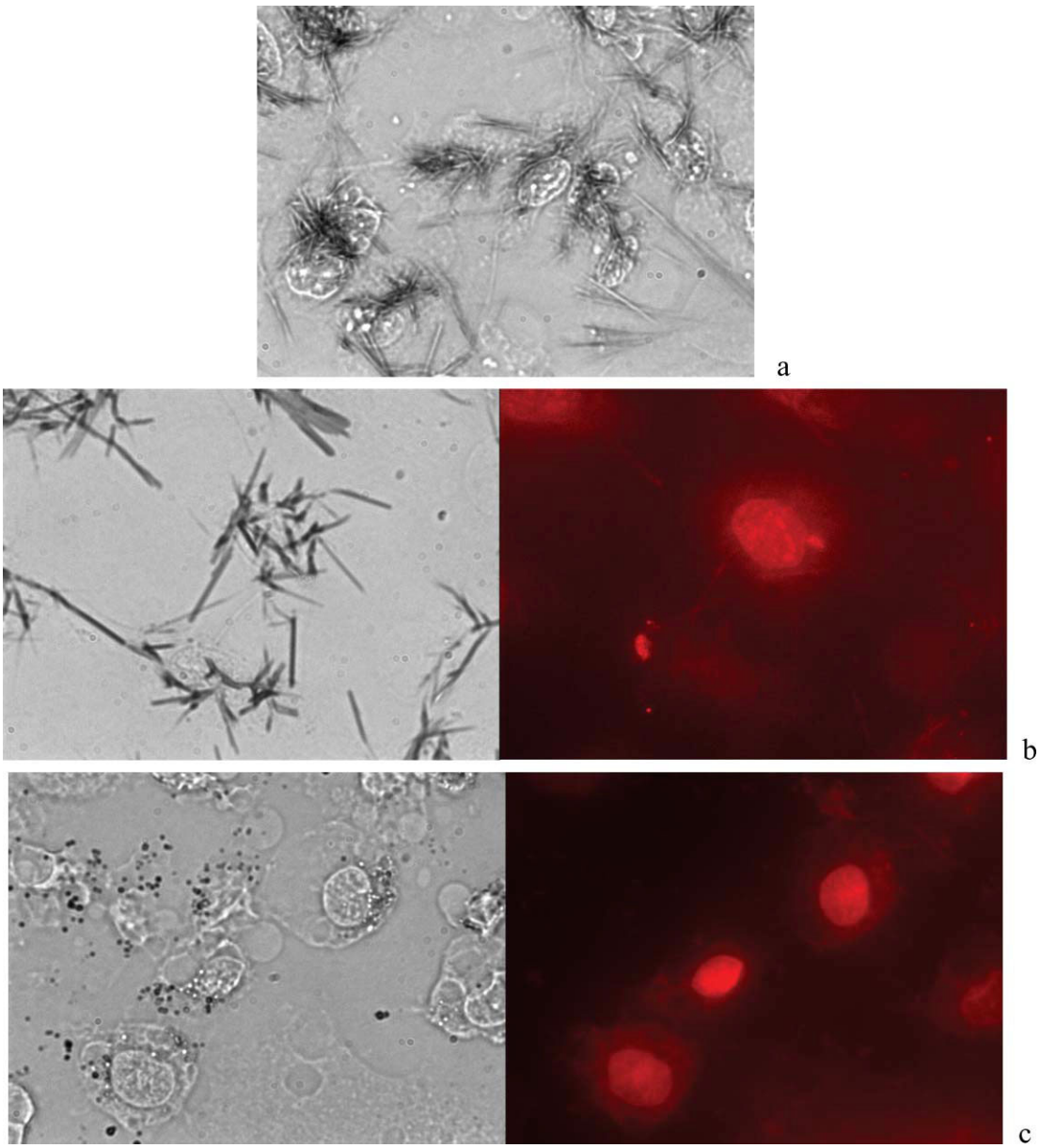

Fig. 6 (a) Bright field image of HeLa cells maintained in the culture medium clearly showing the formation of extracellular formazan crystals in the MTT assay. (b) Images of HeLa cells that contain TMPyP and that are maintained in the culture medium. The left panel is a bright field image showing the formation of extracellular formazan crystals in the MTT assay. The right panel is a corresponding image based on the fluorescence of TMPyP showing that the dye is indeed incorporated into the cells and preferentially localized in the nucleus. (c) Images of HeLa cells that contain TMPyP and that are in SMM. The left panel is a bright field image that shows the formation of formazan granules in the MTT assay. These granules appear to be located inside the cell. The right panel is a corresponding image based on the fluorescence of TMPyP showing that the dye is incorporated into the cells. All bright field images were recorded 4 h after introduction of MTT.

use of D_2O, or mixtures of D_2O in H_2O, to increase the quantum efficiency of singlet oxygen phosphorescence. This point is clearly illustrated with the time-resolved data shown in Fig. 8(b) that were recorded from cells that had been incubated with 15% H_2O (*i.e.*, 8.3 M H_2O). Nevertheless, the data recorded herein all indicate that, upon extrapolation to a H_2O-containing cell, one would observe a singlet oxygen lifetime of ~3 μs. This result is consistent with data we have previously published. (It is important to note that our present time-resolved traces were recorded using sampling windows on the photon-counter that are narrower than those used in our earlier studies.[18] Although these narrower windows allow us to better resolve faster-decaying signals, it also means that, for a given sampling period, our signal-to-noise ratio will be poorer.[29])

When analyzing time-resolved phosphorescence signals from singlet oxygen produced in a photosensitized process, both the ease and accuracy with which the singlet oxygen lifetime can be extracted depends on the relative rates of singlet oxygen formation and decay. In particular, if the rate of singlet oxygen formation is much slower than the rate of decay, then it is necessary to independently quantify this formation rate and deconvolute the

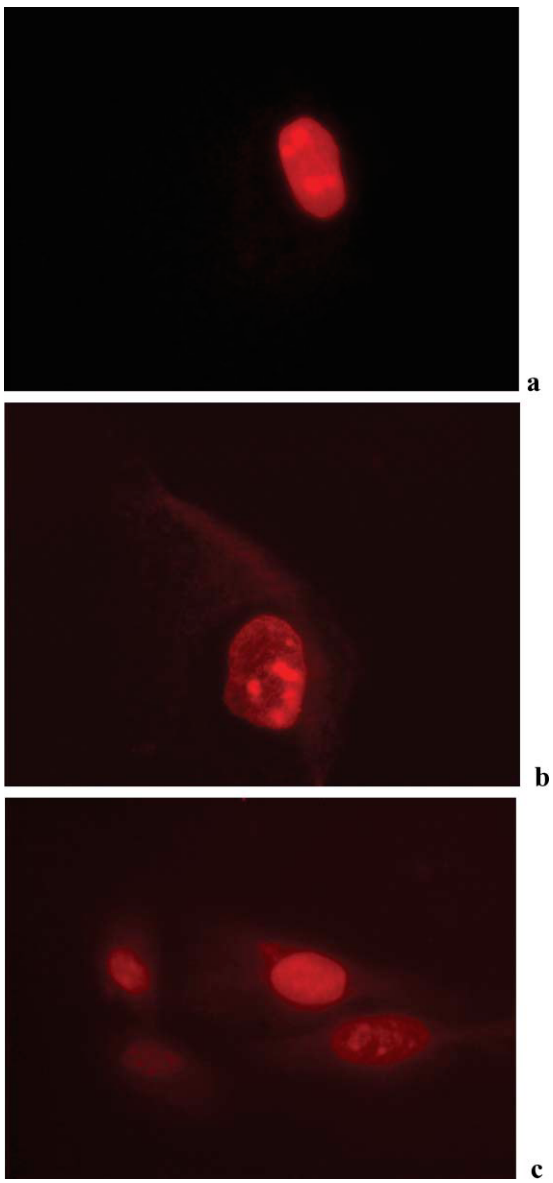

Fig. 7 Example of data obtained from the fast halo assay (FHA) performed on HeLa cells. The images are based on the fluorescence of PI that had been added to stain the DNA. (a) Test performed on a cell that had undergone osmotic shock and that had been exposed to D_2O-based SMM for 5 h. A distinct halo-free fluorescent nucleus is observed, and discrete sub-nuclear structures fluoresce most brightly. (b) As in panel (a), test performed on a cell that had undergone osmotic shock and that had been exposed to SMM for 5 h. The oval-shaped object in the lower center of the figure is the nucleus. The most intense fluorescence is observed from discrete sub-nuclear structures. A dim "halo" can be seen immediately to the right of the nucleus and extending to the upper left corner of the figure. (c) Test performed on cells that had been incubated with TMPyP for 24 h. Halos that are somewhat more distinct are observed in this case.

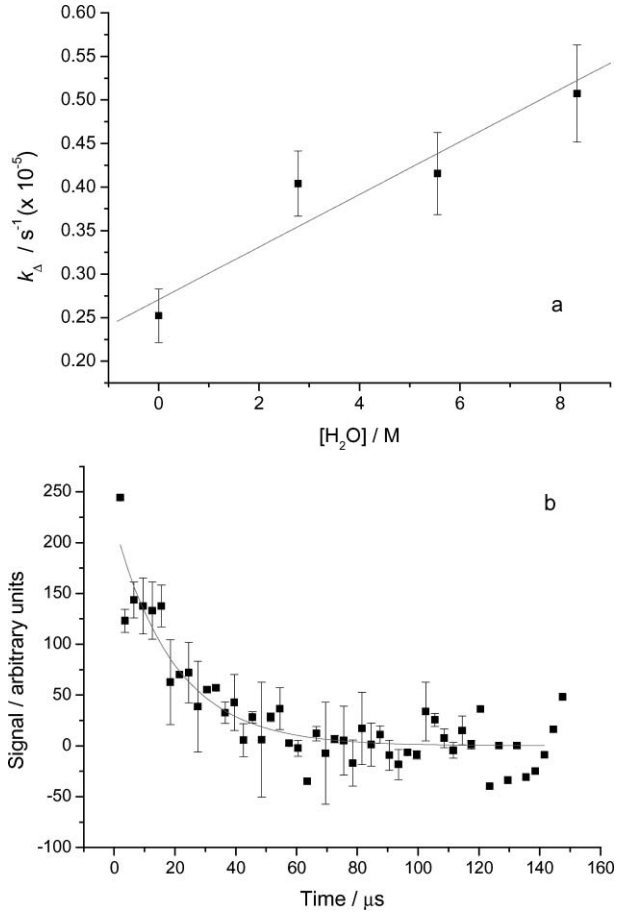

Fig. 8 (a) Plot of the overall rate constant for singlet oxygen deactivation, k_Δ, in single rat neurons against the concentration of H_2O present in the D_2O–H_2O mixture with which the neurons had been incubated. The comparatively large error bars on the data points reflect the signal-to-noise ratio in the time-resolved singlet oxygen phosphorescence data from the cell. (b) Time-resolved singlet oxygen phosphorescence signal from the cell where averaged data recorded from two cells containing 8.3 M H_2O are shown. The solid line is a single exponential fit to the data.

corresponding time profile from the observed singlet oxygen phosphorescence signal to obtain the intrinsic singlet oxygen lifetime.[18,22,46] In an earlier study, we examined this issue with respect to singlet oxygen phosphorescence recorded from single cells.[18] On the basis of data obtained upon irradiation into the nucleus of TMPyP-containing cells that were maintained in the minimal medium (*i.e.*, MMM), we felt it was appropriate to analyze the observed phosphorescence signal using a singlet oxygen formation time constant of ~3 μs.[18] This yielded a singlet oxygen lifetime of 25 ± 2 μs in a neuron that had been incubated in D_2O. In the present studies, however, where the cells were maintained in a physiologically compatible medium (SMM) and where we use narrower sampling windows for better time-resolution (*vide supra*), we have yet to find evidence of a correspondingly slow time constant of singlet oxygen formation upon irradiation into the nucleus of a TMPyP-containing cell. With respect to raw numbers, this simply means that the singlet oxygen lifetime we obtain for a D_2O-incubated cell in the present study (τ_Δ = 36 ± 2 μs) is slightly longer than that estimated in our earlier studies (of course, these respective values of τ_Δ will also reflect residual intracellular H_2O that was not removed in the D_2O/H_2O exchange). In any event, this difference is small, and becomes effectively meaningless when extrapolating to the case of an H_2O-incubated cell where the expected lifetime is still on the order of ~3 μs.

On the other hand, it is reasonable to consider potential changes in the rate of singlet oxygen formation as a function of both the condition of the cell and the amount of light to which the cell has been exposed. Specifically, the sensitizer TMPyP tends to localize in the nucleus and binds to DNA in a number of different ways.[24,47,48] More importantly, these respective TMPyP-DNA complexes are photolabile and exhibit different photophysical properties, including differences in both the yield and kinetics of photosensitized singlet oxygen formation.[24,47] As such, for TMPyP-containing cells in different photosensitized experiments, singlet oxygen could indeed be produced at different rates and in different yields. This is only one point that needs to be considered further in a more extensive study of singlet oxygen production in cells.

In any event, we can categorically say that only a moderate amount of singlet oxygen quenching is observed in a D_2O-incubated cell. It is this result that leads to the more general statement that singlet oxygen in a cell is best characterized as a selective rather than reactive intermediate. This is important not only in considering roles played by singlet oxygen in cell signaling and cell death, but also as one considers methods to exert control over singlet oxygen in biological systems.[49]

Photoinduced cell death

With the results presented in this report, we demonstrate that it is possible to use a variety of probes to monitor events pertinent to light-induced, singlet-oxygen-mediated cell death at the level of a single cell. The data in Fig. 3 nicely illustrate one subtle event that can be monitored and that needs to be investigated further. The Rh123 assay shows that irradiating a cell into which TMPyP has been incorporated causes a loss of the mitochondrial trans-membrane potential which is manifest as a diffuse Rh123 fluorescence and an increase in Rh123 fluorescence from the nucleus (Fig. 3(b) and Fig. 3(c)). Perhaps the most beautiful, albeit fortuitous, aspect of this particular experiment is that the adjacent cell in our image did not take-up TMPyP and served as an intrinsic control in which the mitochondrial trans-membrane potential was not disturbed upon irradiation.

The data in Fig. 3 clearly indicate that it is possible to start measurements of irradiation-induced cell death using cells that are viable. Moreover, we are now able to record singlet oxygen phosphorescence data from a single cell in time periods that range from ~4 s (an integrated intensity) to ~10 min (a time-resolved decay trace). These times are short compared to the time course of, for example, photo-induced apoptotic death (~3–24 h, depending on conditions[50]). Thus, we can begin to correlate spatial and temporal profiles of singlet oxygen in a cell with a tendency for the cell to undergo apoptotic death. The extent to which such singlet oxygen measurements themselves constitute a perturbation of the cell is certainly an issue that must also be investigated. Unlike the data shown in Fig. 3(b) and Fig. 3(c), however, these studies of photo-induced perturbations will be facilitated through the use of spatially-resolved focused laser irradiation in which incident powers can be carefully regulated.

As we embark on this next round of studies, we will also need to incorporate even more stringent control of other conditions under which our experiments are performed. In particular, we must now also consider both the ambient atmosphere and temperature to which the cells are exposed during the optical experiments. In our singlet oxygen phosphorescence measurements thus far, the cells have generally been exposed to an atmosphere of 100% oxygen simply to increase the intensity of the signal being monitored. In the future, we will clearly need to work with cells exposed to oxygen at levels which are typically present in tissue (~5–10% oxygen). Although the corresponding decrease in singlet oxygen phosphorescence intensity will provide an extra experimental challenge, this change in the ambient atmosphere eliminates one potentially complicating perturbative stress to which the cells will respond. Similarly, we need to preclude a potential temperature-induced perturbation. At present, measurements are performed on a microscope stage that is at room temperature (typically 20–22 °C). In the future, cells will be maintained at 37 °C during all measurements.

Conclusions

Time-resolved singlet oxygen phosphorescence experiments were performed on single cells maintained in a HEPES-based, standard physiological buffer. For these cells, an osmotic shock procedure was used to replace intracellular H_2O with D_2O to facilitate the detection of the singlet oxygen phosphorescence. Viability of the cells was confirmed using four assays. In photosensitized experiments performed on metabolically-functioning cells, the lifetime of singlet oxygen in a neuron was found to be the same as that in a HeLa cell. Moreover, these lifetimes for intracellular singlet oxygen are significantly longer than what has commonly been believed for the past 25 years. The present singlet oxygen results are consistent with data previously recorded in our laboratories using cells that were maintained in a less-supportive, non-buffered medium. The data reported herein also demonstrate that it is possible to use a variety of probes, including the phosphorescence of singlet oxygen, to monitor spatially-resolved events pertinent to the light-induced, singlet-oxygen-mediated death of a single cell.

Acknowledgements

This work was supported by the Danish National Research Foundation under a block grant for the Center for Oxygen Microscopy and Imaging. We thank Puk Lund for preparing the cell cultures and Lars Poulsen for assistance in the construction of the microscope used for the fluorescence images.

References

1 C. S. Foote, Mechanisms of photosensitized oxidation, *Science*, 1968, **162**, 963–970.
2 C. S. Foote and E. L. Clennan, *Properties and Reactions of Singlet Dioxygen in Active Oxygen in Chemistry*, ed. C. S. Foote, J. S. Valentine, A. Greenberg and J. F. Liebman, Chapman and Hall, London, 1995, pp. 105–140.
3 *Singlet Oxygen*, ed. A. A. Frimer, CRC Press, Boca Raton, 1985.
4 *Singlet Oxygen*, ed. H. H. Wasserman and R. W. Murray, Academic Press, New York, 1979.
5 H. K. Ledford and K. K. Niyogi, Singlet oxygen and photo-oxidative stress management in plants and algae, *Plant, Cell Environ.*, 2005, **28**, 1037–1045.
6 R. W. Redmond and I. E. Kochevar, Spatially-Resolved Cellular Responses to Singlet Oxygen, *Photochem. Photobiol.*, 2006, **82**, 1178–1186.

7 I. E. Kochevar, M. C. Lynch, S. Zhuang and C. R. Lambert, Singlet oxygen, but not oxidizing radicals, induces apoptosis in HL-60 cells, *Photochem. Photobiol.*, 2000, **72**, 548–553.
8 K. R. Weishaupt, C. J. Gomer and T. J. Dougherty, Identification of Singlet Oxygen as the Cytotoxic Agent in Photo-Inactivation of a Murine Tumor, *Cancer Res.*, 1976, **36**, 2326–2329.
9 T. J. Dougherty, C. J. Gomer, B. W. Henderson, G. Jori, D. Kessel, M. Korbelik, J. Moan and Q. Peng, Photodynamic therapy, *J. Natl. Cancer Inst.*, 1998, **90**, 889–905.
10 M. R. Hamblin and T. Hasan, Photodynamic Therapy: A New Antimicrobial Approach to Infectious Disease?, *Photochem. Photobiol. Sci.*, 2004, **3**, 436–450.
11 J. Mosinger, O. Jirsak, P. Kubat, K. Lang and B. Mosinger, Bactericidal Nanofabrics based on Photoproduction of Singlet Oxygen, *J. Mater. Chem.*, 2007, **17**, 164–166.
12 A. A. Gorman and M. A. J. Rodgers, Current Perspectives of Singlet Oxygen Detection in Biological Environments, *J. Photochem. Photobiol., B*, 1992, **14**, 159–176.
13 A. Baker and J. R. Kanofsky, Time-resolved studies of singlet oxygen emission from L1210 leukemia cells labeled with 5-(*N*-hexadecanoyl)amino eosin. A comparison with a one-dimensional model of singlet oxygen diffusion and quenching, *Photochem. Photobiol.*, 1993, **57**, 720–727.
14 M. Niedre, M. S. Patterson and B. C. Wilson, Direct near-infrared luminescence detection of singlet oxygen generated by photodynamic therapy in cells *In Vitro* and tissues *In Vivo*, *Photochem. Photobiol.*, 2002, **75**, 382–391.
15 I. Zebger, J. W. Snyder, L. K. Andersen, L. Poulsen, Z. Gao, J. D. C. Lambert, U. Kristiansen and P. R. Ogilby, Direct Optical Detection of Singlet Oxygen from a Single Cell, *Photochem. Photobiol.*, 2004, **79**, 319–322.
16 E. Skovsen, J. W. Snyder, J. D. C. Lambert and P. R. Ogilby, Lifetime and Diffusion of Singlet Oxygen in a Cell, *J. Phys. Chem. B*, 2005, **109**, 8570–8573.
17 J. W. Snyder, E. Skovsen, J. D. C. Lambert and P. R. Ogilby, Subcellular, time-resolved studies of singlet oxygen in single cells, *J. Am. Chem. Soc.*, 2005, **127**, 14558–14559.
18 J. W. Snyder, E. Skovsen, J. D. C. Lambert, L. Poulsen and P. R. Ogilby, Optical Detection of Singlet Oxygen from Single Cells, *Phys. Chem. Chem. Phys.*, 2006, **8**, 4280–4293.
19 A. Michaeli and J. Feitelson, Reactivity of Singlet Oxygen Toward Proteins: The Effect of Structure in Basic Pancreatic Trypsin Inhibitor and in Ribonuclease A, *Photochem. Photobiol.*, 1997, **65**, 309–315.
20 P. R. Ogilby and C. S. Foote, The effect of solvent, solvent isotopic substitution, and temperature on the lifetime of singlet molecular oxygen, *J. Am. Chem. Soc.*, 1983, **105**, 3423–3430.
21 M. A. J. Rodgers and P. T. Snowden, Lifetime of $O_2(a^1\Delta_g)$ in Liquid Water as Determined by Time-Resolved Infrared Luminescence Measurements, *J. Am. Chem. Soc.*, 1982, **104**, 5541–5543.
22 S. Y. Egorov, V. F. Kamalov, N. I. Koroteev, A. A. Krasnovsky, B. N. Toleutaev and S. V. Zinukov, Rise and decay kinetics of photosensitized singlet oxygen luminescence in water. Measurements with nanosecond time-correlated single photon counting technique, *Chem. Phys. Lett.*, 1989, **163**, 421–424.
23 R. Schmidt and E. Afshari, Collisional deactivation of $O_2(^1\Delta_g)$ by solvent molecules. Comparative experiments with $^{16}O_2{}^{18}O_2$, *Ber. Bunsen-Ges. Phys. Chem.*, 1992, **96**, 788–794.
24 J. W. Snyder, J. D. C. Lambert and P. R. Ogilby, 5,10,15,20-Tetrakis(*N*-Methyl-4-Pyridyl)-21*H*,23*H*-Porphine (TMPyP) as a Sensitizer for Singlet Oxygen Imaging in Cells: Characterizing the Irradiation-Dependent Behavior of TMPyP in a Single Cell, *Photochem. Photobiol.*, 2006, **82**, 177–184.
25 U. Kristiansen and J. D. C. Lambert, Benzodiazepine and barbiturate ligands modulate responses of cultured hippocampal neurones to the GABA receptor partial agonist, 4-PIOL, *Neuropharmacology*, 1996, **35**, 1181–1191.
26 W.-M. Dai, J. Egebjerg and J. D. C. Lambert, Characteristics of AMPA receptor-mediated responses of cultured cortical and spinal cord neurones and their correlation to the expression of glutamate receptor subunits, GluR1–4, *Br. J. Pharmacol.*, 2001, **132**, 1859–1875.
27 P. Sestili, C. Martinelli and V. Stocchi, The fast halo assay: An improved method to quantify genomic DNA strand breakage at the single-cell level, *Mutat. Res.*, 2006, **607**, 205–214.
28 G. Nikkhah, J. C. Tonn, O. Hoffmann, H.-P. Kraemer, J. L. Darling, R. Schönmayr and W. Schachenmayr, The MTT Assay for Chemosensitivity Testing of Human Tumors of the Central Nervous System, *J. Neuro-Oncol.*, 1992, **13**, 1–11.
29 E. Skovsen, J. W. Snyder and P. R. Ogilby, Two-photon singlet oxygen microscopy: the challenges of working with single cells, *Photochem. Photobiol.*, 2006, **82**, 1187–1197.
30 D. Voet and J. G. Voet, *Biochemistry*, John Wiley and Sons, New York, 2004.
31 N. E. Good, G. D. Winget, W. Winter, T. N. Connolly, S. Izawa and R. Singh, M. M, Hydrogen Ion Buffers for Biological Research, *Biochemistry*, 1966, **5**, 467–477.
32 B. M. Monroe, Quenching of singlet oxygen by aliphatic amines, *J. Phys. Chem.*, 1977, **81**, 1861–1864.
33 E. A. Ogryzlo and C. W. Tang, Quenching of oxygen ($^1\Delta_g$) by amines, *J. Am. Chem. Soc.*, 1970, **92**, 5034–5036.
34 Z. Darzynkiewicz, G. Juan, X. Li, W. Gorczyca, T. Murakami and F. Traganos, Cytometry in Cell Necrobiology: Analysis of Apoptosis and Accidental Cell Death (Necrosis), *Cytometry*, 1997, **27**, 1–20.
35 L. V. Johnson, M. L. Walsh and L. B. Chen, Localization of Mitochondria in Living Cells with Rhodamine 123, *Proc. Natl. Acad. Sci. USA*, 1980, **77**, 990–994.
36 Y. Liu, D. A. Peterson, H. Kimura and D. Schubert, Mechanism of Cellular 3-(4,5-Dimethylthiazol-2-yl)-2,5-Diphenyltetrazolium Bromide (MTT) Reduction, *J. Neurochem.*, 1997, **69**, 581–593.
37 http://www.itl.nist.gov/div898/handbook/prc/section4/prc43.htm.
38 G. N. Georgiou, M. T. Ahmet, A. Houlton, J. Silver and R. J. Cherry, Measurement of the Rate of Uptake and Subcellular Localization of Porphyrins in Cells using Fluorescence Digital Imaging Microscopy, *Photochem. Photobiol.*, 1994, **59**, 419–422.
39 http://rsb.info.nih.gov/ij/.
40 B. Alberts, A. Johnson, J. Lewis, M. Raff, K. Roberts and P. Walter, *Molecular Biology of the Cell*, Garland Science, New York, 2002.
41 M. H. Heggeness, M. Simon and S. J. Singer, Association of Mitochondria with Microtubules in Cultured Cells, *Proc. Natl. Acad. Sci. USA*, 1978, **75**, 3863–3866.
42 G. Capranico, F. Ferri, M. V. Fogli, A. Russo, L. Lotito and L. Baranello, The effects of camptothecin on RNA polymerase II transcription: Roles of DNA topoisomerase I, *Biochimie*, 2007, **89**, 482–489.
43 R. J. Fiel, Porphyrin-Nucleic Acid Interactions: A Review, *J. Biomol. Struct. Dyn.*, 1989, **6**, 1259–1274.
44 L. G. Marzilli, Medical Aspects of DNA-Porphrin Interactions, *New J. Chem.*, 1990, **14**, 409–420.
45 J. W. Snyder, I. Zebger, Z. Gao, L. Poulsen, P. K. Frederiksen, E. Skovsen, S. P. McIlroy, M. Klinger, L. K. Andersen and P. R. Ogilby, Singlet Oxygen Microscope: From Phase-Separated Polymers to Single Biological Cells, *Acc. Chem. Res.*, 2004, **37**, 894–901.
46 R. L. Clough, M. P. Dillon, K.-K. Iu and P. R. Ogilby, Behavior of Singlet Molecular Oxygen ($^1\Delta_g$) in a Polymer Matrix: Effects of Temperature, Matrix Rigidity, and Molecular Composition, *Macromolecules*, 1989, **22**, 3620–3628.
47 N. N. Kruk, B. M. Dzhagarov, V. A. Galievsky, V. S. Chirvony and P.-Y. Turpin, Photophysics of the cationic 5,10,15,20-tetrakis-(4-*N*-methylpyridyl) porphyrin bound to DNA, $[poly(dA\text{-}dT)]_2$ and $[poly(dG\text{-}dC)]_2$: Interaction with molecular oxygen studied by porphyrin triplet-triplet absorption and singlet oxygen luminescence, *J. Photochem. Photobiol., B*, 1998, **42**, 181–190.
48 I. Borissevitch and S. Gandini, Photophysical studies of excited state characteristics of meso-tetrakis-(4-*N*-methylpyridiniumyl) porphyrin bound to DNA, *J. Photochem. Photobiol., B*, 1998, **43**, 112–120.
49 E. Cló, J. W. Snyder, P. R. Ogilby and K. V. Gothelf, Control and Selectivity of Photosensitized Singlet Oxygen Production: Challenges in Complex Biological Systems, *ChemBioChem*, 2007, **8**, 475–481.
50 N. L. Oleinick, R. L. Morris and I. Belichenko, The Role of Apoptosis in Response to Photodynamic Therapy: What, where, why, and how, *Photochem. Photobiol. Sci.*, 2002, **1**, 1–21.

